Inorg. Chem. **2004**, *43*, 1403–1410

Stabilization of New Forms of the Intermetallic Phases β-$RENiGe_2$ (RE = Dy, Ho, Er, Tm, Yb, Lu) in Liquid Indium

J. R. Salvador,[†] J. R. Gour,[†] D. Bilc,[‡] S. D. Mahanti,[‡] and M. G. Kanatzidis*[,†]

Department of Chemistry and Center for Fundamental Materials Research, Michigan State University, East Lansing, Michigan 48842, and Department of Physics and Astronomy and Center for Fundamental Materials Research, Michigan State University, East Lansing, Michigan 48842

Received November 11, 2003

Flux conditions using liquid indium bypass the thermodynamically stable structure and yield new forms of the phases $RENiGe_2$ (RE = Dy, Er, Yb, Lu). The compounds crystallize in the orthorhombic *Immm* space group and possess the $YIrGe_2$ structure type. Lattice parameters for $ErNiGe_2$, $DyNiGe_2$, $YbNiGe_2$, and $LuNiGe_2$ are a = 4.114(1) Å, b = 8.430(2) Å, c = 15.741(5) Å; a = 4.1784(9) Å, b = 8.865(2) Å, c = 15.745(3) Å; a = 4.0935(6) Å, b = 8.4277(13) Å, c = 15.751(2) Å, and a = 4.092(1) Å, b = 8.418(3) Å, c = 15.742(5) Å, respectively. These phases represent a new structural arrangment (β) of the compound type $RENiGe_2$ as another set of compounds with identical stoichiometry are known to adopt the orthorhombic *Cmcm* $CeNiSi_2$ type structure (α). In this paper we report the crystal and electronic band structure of four new members of the $YIrGe_2$ structure type, as well as an investigation of the relative thermodynamic stabilities of the two forms.

Introduction

In recent years we and others have used molten metal fluxes for the exploratory synthesis of intermetallic compounds with a great deal of success. Specifically, molten Al and Ga fluxes have shown themselves to be excellent routes to complex ternary and quaternary intermetallic phases of the type RE/M/Al[1] and RE/M/Si,Ge[2] when Al is used as the solvent, and RE/M/Ga,[3] RE/M/Si,[4] RE/M/Ga/Si,Ge,[5] RE/Ga/Ge[6] when Ga is used as the solvent (where RE = Y, La−Lu, M = a transition metal). One of the advantages of using these fluxes is that the products often form as large high quality crystals, which facilitates the structural and physical characterization of these new compounds.

Given the success of molten Al and Ga in forming new compounds, it seems the next logical step would be to employ indium as a flux for the synthesis of intermetallic compounds, since it has many of the characteristics that make Al and Ga excellent candidates for such applications. Particularly attractive is the capacity to dissolve Si, Ge, and a host of lanthanide and transition metals, which results in highly reactive forms of the elements. Further, indium does not form binaries with Ge or Si and possesses a low melting point of 156 °C.[7] A quick review of the literature shows only a handful of examples of indium being used as flux, and so this area is relatively unexplored.[8]

One of the most important findings from our exploration of molten metals as solvents was that some compounds can only be formed via flux synthesis, and either cannot be obtained or are very difficult to obtain by more conventional

* To whom correspondence should be addressed. E-mail: kanatzid@cem.msu.edu.

[†] Department of Chemistry and Center for Fundamental Materials Research.

[‡] Department of Physic and Astronomy and Center for Fundamental Materials Research.

(1) (a) Fehrmann, B.; Jeitschko, W. *J. Alloys Compd.* **2000**, *298*, 153. (b) Thiede, V. M. T.; Fehrmann, B.; Jeitschko, W. *Z. Anorg. Allg. Chem.* **1999**, *625*, 1417.

(2) (a) Sieve, B.; Trikalitis, P. N.; Kanatzidis M. G. *Z. Anorg. Allg. Chem.* **2002**, *628*, 1568. (b) Sieve, B.; Sportouch, S.; Chen, X. Z.; Cowen, J. A.; Brazis, P.; Kannewurf, C. R.; Papaefthymiou, V.; Kanatzidis M. G. *Chem. Mater.* **2001**, *13*, 273. (c) Latturner, S. E.; Bilc, D.; Mahanti S. D.; Kanatzidis M. G. *Chem. Mater.* **2002**, *14*, 1695.

(3) (a) Chen, X. Z.; Small, P.; Sportouch, S.; Zhuravleva, M.; Brazis, P.; Kannewurf, C. R.; Kanatzidis, M. G. *Chem. Mater.* **2000**, *12*, 2520. (b) Schluter, M.; Jeitschko, W. *Inorg Chem.* **2001**, *40*, 6362.

(4) Chen, X. Z.; Larson, P.; Sportouch, S.; Brazis, P.; Mahanti, S. D.; Kannewurf, C. R.; Kanatzidis, M. G. *Chem. Mater.* **1999**, *11*, 75.

(5) Zhuravleva, M. A.; Chen, X. Z.; Wang, X. P.; Schultz, A. J.; Ireland J.; Kannewurf, C. R.; Kanatzidis, M. G. *Chem. Mater.* **2002**, *14*, 3066.

(6) Bryan, J. D.; Stucky, G. D. *Chem. Mater.* **2000**, *13*, 253.

(7) Massalski, T. B. *Binary Alloy Phase Diagrams*, 2nd ed.; ASM International: New York, 1990; Vol. 1, p 484; Vol. 2, p 1856.

(8) (a) Pagliuso, P. G.; Sarrao, J. L.; Thompson, J. D.; Hundley, M. F.; Sercheli, M. S.; Urbano, R. R.; Rettori, C.; Fisk, Z.; Oseroff, S. B. *Phys. Rev. B* **2001**, *63*, art no. 092406-1. (b) Zaremba, V. I.; Kalychak, Y. M.; Tyvanchuk, Y. B.; Hoffmann, R.-D.; Möller, M. H.; Pöttgen, R. *Z. Naturforsch., B: Chem. Sci.* **2002**, *57*, 791. (c) Macaluso, R. T.; Sarrao, J. L.; Pagliuso, P. G.; Moreno, N. O.; Goodrich, R. G.; Browne, D. A.; Fronczek, F. R.; Chan, J. Y. *J. Solid State Chem.* **2002**, *166*, 245.

10.1021/ic035303j CCC: $27.50
Published on Web 01/24/2004

intermetallic reaction techniques such as arc-melting or radio frequency (rf) induction heating of the elements.[9] That is to say that certain compounds are stabilized by the flux, either by virtue of the chemical environment provided by the molten metal or simply because the reactions are being carried out in a lower temperature regime, making it possible to trap phases that are kinetically stable.

We report here the stabilization of a new form of the compounds $RENiGe_2$ (RE = Dy, Er, Yb, Lu) which crystallize in the orthorhombic *Immm* space group with the $YIrGe_2$ structure type.[10] There have been many reported members of this structure type with compositions $REMGe_2$ (RE = Tb−Lu, Y, M = Ir, Pd, Pt), and many of these have been characterized by magnetic neutron diffraction and possess complex magnetically ordered structures.[11] All of these phases, however, contain second row transition metals and were produced by arc-melting of the elements with the exception of $EuIrGe_2$ which crystallizes in the $CeNiSi_2$ structure type.[12] If, on the other hand, one arc-melts Er, Dy, Yb, or Lu, with first row transition metals such as Ni, and Ge in 1:1:2 ratio, a different structure is obtained, namely compounds with the $CeNiSi_2$ structure type.[13] The title compounds contain first row transition metals but adopt the $YIrGe_2$ structure type. They can only be produced by an indium flux reaction of the elements, which suggests that this new form (henceforth referred to as the β-form) of $RENiGe_2$ is a kinetically stable phase. Here we show that the $CeNiSi_2$-type form (henceforth referred to as the α-form) is the thermodynamically stable form.

Experimental Section

Synthesis. $ErNiGe_2$, $HoNiGe_2$, $DyNiGe_2$, $TmNiGe_2$, $YbNiGe_2$, and $LuNiGe_2$ were prepared by combining 1.0 mmol of rare earth metal Er (5−10 mm ribbons, 99.6%, Research Chemicals, Phoenix, AZ), Ho (250 mesh powder 99.9% Cerac Milwaukee, WI), Dy (sponge 99.6%, Research Chemicals, Phoenix AZ), Tm (metal chunk, 99.9%, Chinese Rare Earth Information Center, Inner Mongolia, China), Yb (metal chunk, 99.9%, Chinese Rare Earth Information Center, Inner Mongolia, China), and Lu (−40 mesh 99.9% Cerac Milwaukee WI), 1.0 mmol of Ni (−325 mesh 99.9% Cerac Milwaukee WI), and 2.0 mmol of Ge (2−5 mm pieces 99.99% Plasma Materials Livermore, CA) and 10.0 mmol of indium (tear drops 99.9 Cerac) in alumina tubes. All reagents were used as received without further purification, and reactions were prepared under an inert N_2 atmosphere in a drybox. It has been found that fine powders of the reactants (excluding In) enhance the yields of β-$RENiGe_2$ The alumina tubes and reactants were then flame-sealed in fused silica tubes under a reduced atmosphere to prevent oxidation during heating. The samples were heated to 1000 °C over 10 h and held for 4 h. The temperature was then ramped down to 850 °C and held for an additional 48 h, then cooled to room temperature over the course of another 48 h. Product isolation from the excess indium was accomplished by centrifugation, where a coarse frit was placed in the open end of the reaction vessel and then resealed under a reduced atmosphere in a Pyrex tube. This was heated to 300 °C to ensure the excess indium was molten, and then the sample was centrifuged for 5 min. This process removed almost all excess indium. Further purification was carried out by a 15 min submersion and sonication in 6 M aqueous HCl. Longer exposure to, or use of higher concentrations of, HCl has a deleterious effect on product crystal quality.

β-$TmNiGe_2$ and β-$HoNiGe_2$ were identified by comparing experimental powder X-ray diffraction patterns with a calculated powder pattern from the refined structure of $ErNiGe_2$. Neither the Tm nor Ho analogues of these phases will form if large chunks (3−5 mm in greatest dimension) of rare-earth metals are used as starting materials, and this is why these phases were not initially found. Their structures were not refined, and no further characterization was performed on them.

Elemental Analysis. Semiquatitative microprobe elemental analysis was performed with a JEOL JSM-35C scanning electron microscope (SEM) equipped with the Noran energy dispersive spectrometer (EDS). Data were acquired using an accelerating voltage of 20 kV and 100 s acquisition times. Several crystals from each reaction were analyzed resulting in approximate atomic ratios of 1:1:2 RE/Ni/Ge. These results agree quite well with the atomic ratios that were derived from the refinement of the crystal structure.

X-ray Crystallography. Single-crystal X-ray diffraction data were collected at room temperature using a Bruker AXS SMART CCD diffractometer with graphite monochromatized Mo Kα (λ = 0.71073 Å) radiation. Unit cell refinement and data merging were done with the SAINT program, and an empirical absorption correction was applied using the program SADABS.[14] Inspection of the systematic absences immediately found the structure to be *I* centered. The condition $h + k + l = 2n$ was the only independent condition found which led to 4 possible space groups *I*222, $I2_12_12_1$, *Imm*2, and *Immm*. *Immm* (No. 71) was the only centrosymmetric choice available and so was chosen.[15] A structural solution was obtained by direct methods using the program SHELXS, and the final structural refinement was completed with the SHELXL suite of programs.[16] The crystal structure refinement data for $DyNiGe_2$, $ErNiGe_2$, $YbNiGe_2$, and $LuNiGe_2$ are given in Table 1. The atomic positions and isotropic displacement parameters for $DyNiGe_2$, $ErNiGe_2$, $YbNiGe_2$, and $LuNiGe_2$ are listed in Table 2. The structure solutions for these compounds indicate fully occupied sites and no disorder, although inspection of the anisotropic displacement parameters, both β-$DyNiGe_2$ and β-$ErNiGe_2$, show a large displacement parameter along the U_{11} direction for Ge(1). This may imply the presence of a weak modulation in the structure. The anisotropic displacement parameters for all compounds have been deposited with the Supporting Information.

(9) (a) Sieve, B.; Chen, X. Z.; Henning, R.; Brazis, P.; Kannewurf, C. R.; Cowen, J. A.; Schultz, A. J.; Kanatzidis, M. G. *J. Am. Chem. Soc.* **2001**, *123*, 7040. (b) Salvador, J. R.; Bilc, D.; Mahanti, S. D.; Kanatzidis, M. G. *Angew. Chem., Intl. Ed.* **2002**, *38*, 844.

(10) Francois, M.; Venturini, G.; McRoe, E.; Malamanx, B.; Roques, B. *J. Less-Common Met.* **1987**, *128*, 249.

(11) (a) Salamakha, P. S.; Sologub, O.; Yakinthos, J. K.; Routis, Ch. D. *J. Alloys Compd.* **1998**, *267*, 192. (b) Gladyshevskii, R. E.; Parthé, E.; Sologub, O. L.; Samalakha, P. S. *Z. Kristallogr.* **1993**, *205*, 321. (c) Gil, A.; Penc, B.; Hofmann, M.; Szytula, A.; Zygmunt, A. *J. Alloys Compd.* **2001**, *322*, 21. (d) Papathanassiou, G.; Kostanidis, P. A.; Yakinthos, J. K.; Schäfer, W. *J. Alloys Compd.* **1999**, *290*, 17. (e) Schmitt, D.; Ouladdiaf, B.; Routsi, C. D.; Yakinthos, J. K.; Gamari-Seale, H. *J. Alloys Compd.* **1999**, *292*, 21.

(12) Pöttgen, R.; Simon, A. *Z. Anorg. Allg. Chem.* **1996**, *622*, 779.

(13) Pecharskii, V. K.; Mruz, O. Ya.; Konyk, M. B.; Salanaka, P. S.; Starodub, P. K.; Fedyna, M. F.; Bodak, O. I. *J. Struct. Chem.* **1989**, *30*, 777.

(14) *SAINT*, version 4; Siemens Analytical X-ray Instruments, Inc.: Madison, WI. Sheldrick, G. M. *SADABS*; University of Göttingen: Göttingen, Germany, 1995.

(15) Hahn, T. *International Table for Cystallography*, 4th ed.; Kluwer Academic: Boston, 1997; Vol. A, pp 45, 314−315.

(16) Sheldrick, G. M. *SHELXTL. Structure Determination Program*, version 5.0; Siemens Analytical X-ray Instruments Inc.: Madison, WI, 1995.

Table 1. Crystallographic Data for RENiGe$_2$ (RE = Dy, Er, Yb, Lu)

empirical formula	$DyNiGe_2$	$ErNiGe_2$	$YbNiGe_2$	$LuNiGe_2$
fw	366.39	371.15	376.93	378.86
cryst syst/space group	orthorhombic/*Immm*	orthorhombic/*Immm*	orthorhombic/*Immm*	orthorhombic/*Immm*
unit cell dimensions (Å)	$a = 4.1784(9)$	$a = 4.114(2)$	$a = 4.0935(6)$	$a = 4.0924(14)$
	$b = 8.8645(19)$	$b = 8.430(5)$	$b = 8.4277(13)$	$b = 8.418(3)$
	$c = 15.745(3)$	$c = 15.741(5)$	$c = 15.751(12)$	$c = 15.742(5)$
V/Z	583.2(2)/8	546.0(5)/8	543.40(14)/8	542.3(3)/8
density(calcd) (g/cm^3)	8.436	9.031	9.215	9.281
abs coeff (mm^{-1})	51.756	58.65	62.466	64.511
θ range for data collection (deg)	2.59−27.01	2.59−27.06	2.59−27.15	4.58−29.58
index ranges	$-5 \le h \le 5$	$-5 \le h \le 2$	$-5 \le h \le 5$	$-5 \le h \le 5$
	$-11 \le k \le 9$	$-10 \le k \le 10$	$-10 \le k \le 10$	$-11 \le k \le 11$
	$-19 \le l \le 20$	$-20 \le l \le 19$	$-20 \le l \le 19$	$-21 \le l \le 19$
reflns collected/unique/R(int)	2522/401/0.0517	1845/387/0.0324	2432/377/0.0602	2261/450/0.0304
data/restraints/params	401/0/30	387/0/30	377/0/30	450/0/30
GOF on F^2	1.266	0.763	1.183	1.060
final R indices [$I > 2\sigma(I)$] (R1/wR2)[a]	0.0421/0.1174	0.0253/0.0855	0.0443/0.1018	0.0231/0.0592
R indices (all data) (R1/wR2)	0.0429/0.1181	0.0266/0.0871	0.0454/0.1033	0.0271/0.0605
extinction coeff	0.0019(3)	0.0047(3)	0.0055(3)	0.00224(15)
largest diff peak and hole (e/Å^3)	3.984 and −4.443	2.080 and −1.942	7.009 and −4.913	3.063 and −2.043

[a] $R1 = \sum||F_o| - |F_c||/\sum|F_o|$ and $wR2 = [\sum(|F_o^2 - F_c^2|)^2/\sum(wF_o^2)^2]^{1/2}$.

Table 2. Atomic Coordinates ($\times 10^4$) and Equivalent Isotropic Displacement Parameters (Å$^2 \times 10^3$) for $DyNiGe_2$, $ErNiGe_2$, $YbNiGe_2$, and $LuNiGe_2$

atom	Wyckoff position	x	y	z	U(eq)[a]
Dy(1)	*4j*	0	1/2	2081(1)	5(1)
Dy(2)	*4g*	0	2831(1)	0	7(1)
Ge(1)	*4i*	0	1/2	4143(1)	11(1)
Ge(2)	*4i*	1/2	1/2	786(2)	6(1)
Ge(3)	*8l*	0	1591(2)	1907(1)	7(1)
Ni(1)	*8l*	0	2352(3)	3466(1)	7(1)
Er(1)	*4j*	0	1/2	2040(1)	5(1)
Er(2)	*4g*	0	2602(1)	0	7(1)
Ge(1)	*4i*	0	1/2	4204(1)	10(1)
Ge(2)	*4i*	1/2	1/2	770(1)	5(1)
Ge(3)	*8l*	0	1568(2)	1958(1)	6(1)
Ni(1)	*8l*	0	2490(2)	3522(1)	6(1)
Yb(1)	*4j*	0	1/2	2033(1)	6(1)
Yb(2)	*4g*	0	2612(1)	0	9(1)
Ge(1)	*4i*	0	1/2	4231(1)	7(1)
Ge(2)	*4i*	1/2	1/2	794(1)	14(1)
Ge(3)	*8l*	0	1570(2)	1966(1)	9(1)
Ni(1)	*8l*	0	2490(2)	3525(1)	8(1)
Lu(1)	*4j*	0	1/2	2034(1)	5(1)
Lu(2)	*4g*	0	2615(1)	0	7(1)
Ge(1)	*4i*	0	1/2	4228(1)	5(1)
Ge(2)	*4i*	1/2	1/2	795(1)	11(1)
Ge(3)	*8l*	0	1568(2)	1966(1)	6(1)
Ni(1)	*8l*	0	2484(2)	3526(1)	6(1)

[a] U(eq) is defined as one-third of the trace of the orthogonalized U^{ij} tensor.

Phase identity and purity of polycrystalline samples was determined by powder X-ray diffraction, carried out with a Rigaku rotating Cu anode diffractometer with post diffraction monochromator.

Other Physical Methods. Differential thermal analysis (DTA) was performed on a Shimadzu DTA-50 differential thermal analyzer.

Magnetic susceptibility measurements were made on hand picked crystals which were ground and screened by powder X-ray diffraction for phase identity and purity. Measurements were performed with a Quantum Design SQUID magnetometer in both field cooled and zero field cooled settings at temperatures between 2 and 300 K with an applied field of 500 Oe. Additionally, magnetization measurements were made from −55 to 55 kOe at 2 K.

Band Structure Calculations. Band structure calculations were performed on both α- and β-$LuNiGe_2$ using the self-consistent full-potential linearized augmented plane wave method (LAPW)[17] within density functional theory (DFT) with a generalized gradient approximation (GGA) for the exchange and correlation potential within the Perdew−Burke−Ernzerhof model.[18] Scalar relativistic corrections were added, and spin−orbit interaction (SOI) was incorporated using a second variational procedure.[19] Calculations were carried out on the Lu system due to the inability of DFT to accurately model the highly correlated electrons found in partially filled f levels. The calculations were performed with the WIEN97 program.[20] The atomic radii values (in atomic units 1 au = 0.529 Å) used in the calculation are as follows: 2.4 for Lu, 2.15 for Ni, and 2.25 for Ge. Self-consistent iterations were performed with 27 k points in the reduced Brillouin zone with a cutoff between valence and core states of −6.0 Ry; convergence was assumed when the total energy difference between cycles was within 0.0001 Ry. Total energy was computed for both α- and β-forms of the structure by a full volume relaxation method in which the structure is allowed to minimize its energy by relaxing the cell volume and atomic positions.

Results and Discussion

Structure. Despite their stoichiometric equivalence, the structures of the title compounds are distinct from those of the α-form. Figure 1a shows the overall structure of β-$RENiGe_2$ as viewed down the a axis, and Figure 1b shows the structure of the α-form for comparison. Figure 2a shows the structure of the β-phase as viewed down the b axis, and

(17) (a) Hohenberg, H.; Kohn, W. *Phys. Rev.* **1964**, *136*, B864. (b) Kohn, W.; Sham, L. *Phys. Rev.* **1965**, *140*, A1133. (c) Singh, D. *Planewaves, Pseudopotentials, and the LAPW Method*; Kluwer Academic: Boston, 1994.
(18) Perdew, J. P.; Burke, K.; Ernzerhof, M. *Phys. Rev. Lett.* **1996**, *77*, 3865.
(19) Koelling, D. D.; Harmon, B. *J. Phys. C: Solid State Phys.* **1980**, *136*, 147.
(20) Blaha, P.; Schwartz, K.; Luitz, J. *WIEN97, a full potential linearized augmented plane wave package for calculating crystal properties*; Karlhienz Schwartz, Tech. Universität Wien, Austria, 1999.

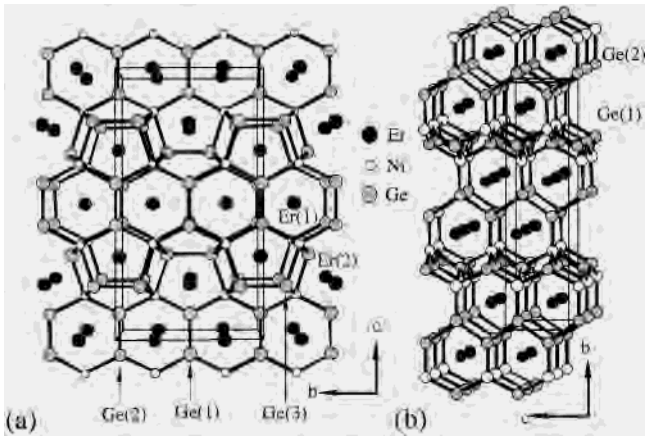

Figure 1. (a) The structure of β-RENiGe$_2$ as viewed down the *a* axis. (b) The overall structure of α-RENiGe$_2$, a perspective view along the *a* axis.

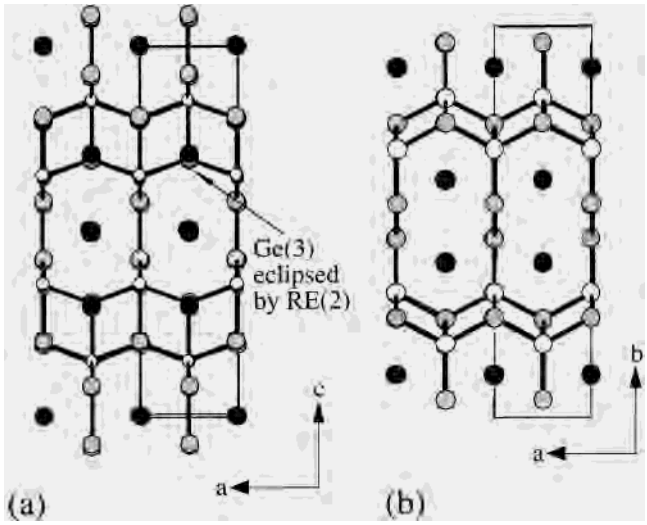

Figure 2. (a) The structure of β-RENiGe$_2$ showing the tunnel that runs along the *b* axis. (b) The structure of α-RENiGe$_2$ as viewed down the *c* axis, which exhibits channels which run along this axis.

Table 3. Bond Lengths [Å] for DyNiGe$_2$, ErNiGe$_2$,YbNiGe$_2$, and LuNiGe$_2$

	RE = Dy	RE = Er	RE = Yb	RE = Lu	
RE(1)−Ge(2)	2.9193(19)	2.8684(18)	2.8554(14)	2.8518(12)	×2
RE(1)−Ge(3)	2.9821(13)	2.9099(14)	2.903(1)	2.8880(14)	×4
RE(1)−Ge(3)	3.0340(19)	2.896(2)	2.8924(14)	2.9013(10)	×2
RE(1)−Ni	3.0746(18)	3.0688(16)	3.0573(12)	3.0554(11)	×4
RE(2)−Ge(1)	3.0340(19)	3.1282(13)	3.1159(9)	3.1139(9)	×4
RE(2)−Ge(2)	3.0975(12)	3.2581(14)	3.255(1)	3.2551(9)	×2
RE(2)−Ge(3)	3.1971(18)	3.204(2)	3.2179(3)	3.2162(14)	×2
RE(2)−Ni	3.1976(18)	3.1068(18)	3.0979(15)	3.0948(12)	×4
Ge(1)−Ni	2.578(2)	2.373(2)	2.3713(19)	2.3647(14)	×2
Ge(1)−Ge(1)	2.698(4)	2.507(4)	2.423(4)	2.431(3)	
Ge(2)−Ni	2.394(3)	2.394(3)	2.3762(18)	2.3728(14)	×2
Ge(2)−Ge(2)	2.476(5)	2.423(4)	2.500(4)	2.502(3)	
Ge(3)−Ni(1)	2.3637(14)	2.3313(14)	2.328(1)	2.3276(9)	×3
Ge(3)−Ge(3)	2.821(4)	2.643(3)	2.647(3)	2.646(2)	

Figure 2b shows the *c* axis view of the α-phase. The main difference between the two phases is in the distribution of the Ge species. The α-form exists as single Ge atoms and infinite Ge chains, whereas the β-form contains only Ge dimers. A list of the selected bond distances for β-RENiGe$_2$ is found in Table 3. The title compounds are composed of two sets of Ge dimers that are formed by the bonding of

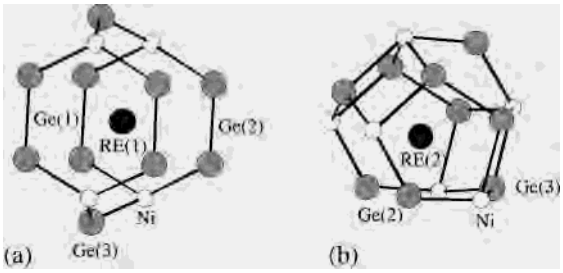

Figure 3. (a) Coordination environment of RE(1) in β-RENiGe$_2$. (b) Coordination environment of RE(2) in β-RENiGe$_2$.

symmetry equivalent atoms between Ge(1)−Ge(1) with lengths of 2.698(4), 2.507(4), 2.423(4), 2.431(3) Å for the Er, Dy, Yb, and Lu compounds, respectively, and Ge(2)−Ge(2) with lengths 2.476(5), 2.423(4), 2.500(4), 2.502(3) Å for Dy, Er, Yb, and Lu, respectively. These Ge dimers then bond to Ni atoms with Ge(1)−Ni distances of 2.578(2), 2.373(2), 2.371(2), 2.3949(18) Å and Ge(2)−Ni distances of 2.394(3), 2.394(3), 2.376(2), 2.365(1)Å for Dy, Er, Yb, and Lu, respectively, forming a distorted Ni_2Ge_4 hexagon. Both Ge(1) and Ge(2) are in a trigonal planar bonding arrangement. The Ni atom forms an additional 3 bonds to Ge(3) atoms at distances of 2.3637(14), 2.3313(14), 2.328(1), 2.3276(9) Å for Dy, Er, Yb, and Lu making for a 5 coordinate square pyramidal geometry. The Ge(3) atoms form another kind of dimer with distances 2.821(4), 2.643(3), 2.647(3), 2.646(2) Å for the Dy, Er, Yb, and Lu analogues, respectively. Therefore, the Ge(3)−Ge(3) dimer is an ethane-like unit with an eclipsed geometry. The result is a three-dimensional [$NiGe_2$] network with channels extending down the *b* axis (Figure 2a), and cages encapsulating the RE atoms. RE(1) resides in the center of the two hexagons created by the Ge(1) and Ge(2) dimers and the capping Ni atoms, Figure 3a. These hexagons define the tunnels which extend down the *a* axis. The RE(2) sites are in a cage composed of Ge(3), Ge(2), and Ni atoms, see Figure 3b. There is a large difference in the bond lengths between the Dy and Er analogues, particularly with the Ge(3)−Ge(3) and Ge(1)−Ge(1) distances. Indeed, the lattice parameters for these compounds differ to a much greater extent than do those of the remaining 3 analogues. This may be caused by the inclusion of a small amount if In into the structure of $DyNiGe_2$. This is not reflected in the single crystal X-ray data, but it may be present in an amount that is not detectable by X-ray.

In contrast to the β-form, the structure of α-RENiGe$_2$ is composed of PbO type layers containing Ni and Ge(2) atoms. These layers are connected through Ni−Ge(1) bonds to zigzag chains of Ge atoms running along the *c* axis. As a result, the Ni atoms are 5 coordinate with square pyramidal geometry, and the Ge(2) atoms within the layer are tetrahedrally coordinated, Figure 1b. This structure also contains channels of RE ions, which run parallel to the *c* axis (Figure 2b).

While the two phases are distinct from one another, a simple scheme to interconvert the two structures can be envisioned in the following way. If one of the Ge(1)−Ni

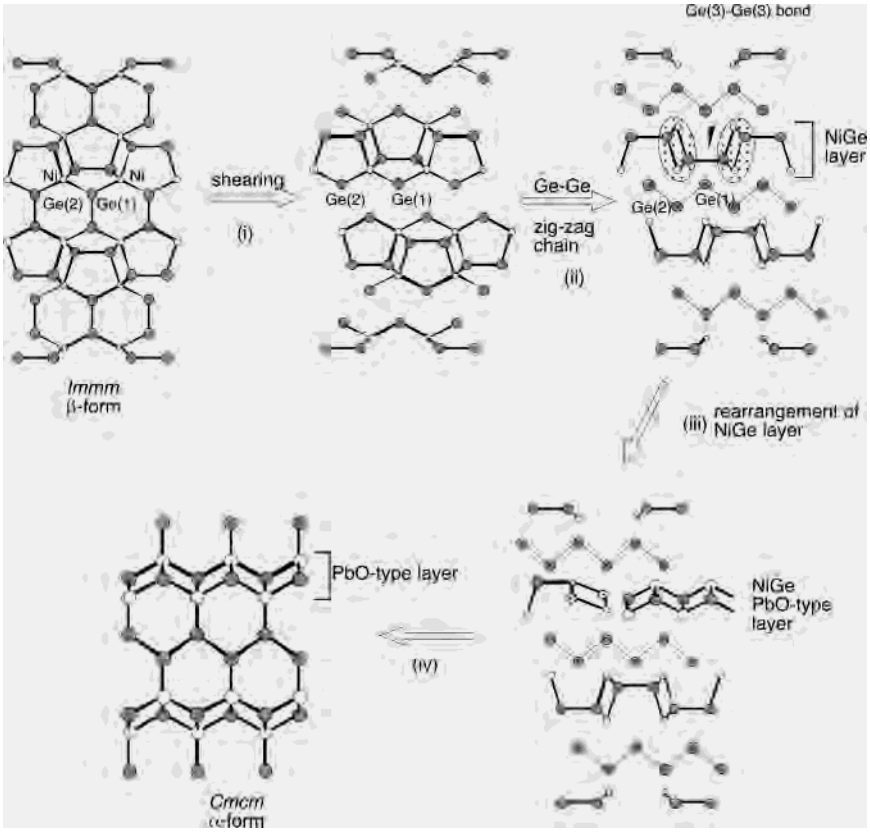

Figure 4. Conceptual stepwise conversion scheme from the β-RENiGe$_2$ structure to the α-form (CeNiSi$_2$ type structure). The shaded ovals after step (ii) need to be rotated to break the Ge(3)−Ge(3) bond and form the PbO-type layer.

and Ge(2)−Ni bonds is broken and the hexagonal slab is sheared along the *b* axis, the Ge dimers will tilt until Ge(1) and Ge(2) can form a bond. This results in a Ge zigzag chain that propagates along the *b* axis, see Figure 4, steps i and ii. Then, if the Ge(3)−Ge(3) bond is broken and new Ge−Ni bonds form with adjacent Ni atoms (by an appropriate rotation of the fragment shown in the shaded areas in Figure 4), this will lead to the compression of the cage layer. This rearrangement will bring about the formation of a new NiGe, PbO-type layer, which could then connect to the zigzag Ge chains to form the CeNiSi$_2$-structure type. The interconversion thus requires the breaking of 2 Ni−Ge bonds and 1 Ge−Ge bond and a substantial amount of atomic reorganization in order to take place. This would suggest a large reorganization barrier, and one may predict on the basis of this that the kinetics of interconversion would be slow.

The first hint that the α-form was the thermodynamically stable form came from inspecting the cell volumes of the α- and β-phases. For α-ErNiGe$_2$ the volume of 2 unit cells is 503.6(3) Å^3 while the unit cell volume of the β-form is 546.0(2) Å^3. Since these volumes contain the same number and type of atoms, it is apparent that the atoms are more closely packed in the α-form indicating stronger bonding and presumably a more energetically favorable arrangement.

Synthesis and Thermal Stability. It is interesting to note that the formation of β-RENiGe$_2$ is exclusive to indium flux synthesis. The yields from these reactions range from 60% to 70%, on the basis of the lanthanide metal, with ∼70% purity. The main impurities were the α-phase and recrystallized Ge. When other methods such as arc-melting or rf furnace heating were used to synthesize RENiGe$_2$, they only led to the α-form. Furthermore, when the length of the reaction was increased from 48 to 96 h the α-phase was the dominant fraction, approximately 65%. Likewise, if the isotherm temperature for the reaction was increased from 850 to 1000 °C a larger fraction of the reaction product, approximately 50−60%, crystallized as the α-form. Two other experiments were also conducted where the elements (Dy or Er, Ni, Ge, and In) were combined in a 1:1:2:10 ratio, and then were arc-melted for 3 min, or heated with an rf furnace for 1 h. Both of these methods which employ much higher temperatures than the flux reaction described in the Experimental Section yielded practically pure α-form despite using excess indium. All of these results indicate that the α-phase is the more thermodynamically stable form, and the β-form is likely the kinetically stable phase.

Differential thermal analysis was performed on the title compounds to see if a β- to α-phase transition could be observed. Both β-ErNiGe$_2$ and β-DyNiGe$_2$ were stable up to 1000 °C.[21] Likewise, annealing samples of pure β-ErNiGe$_2$ at 950 °C for 2 weeks also failed to bring about a change to the α-form. X-ray powder patterns of the annealed product were compared to those taken prior to annealing, and no significant changes were observed. The resistance to convert

(21) The experiments were repeated on the α form with similar results. X-ray powder patterns were taken of the compounds before and after the DTA experiment, and no significant changes in the powder patterns of the α forms nor the β forms were found.

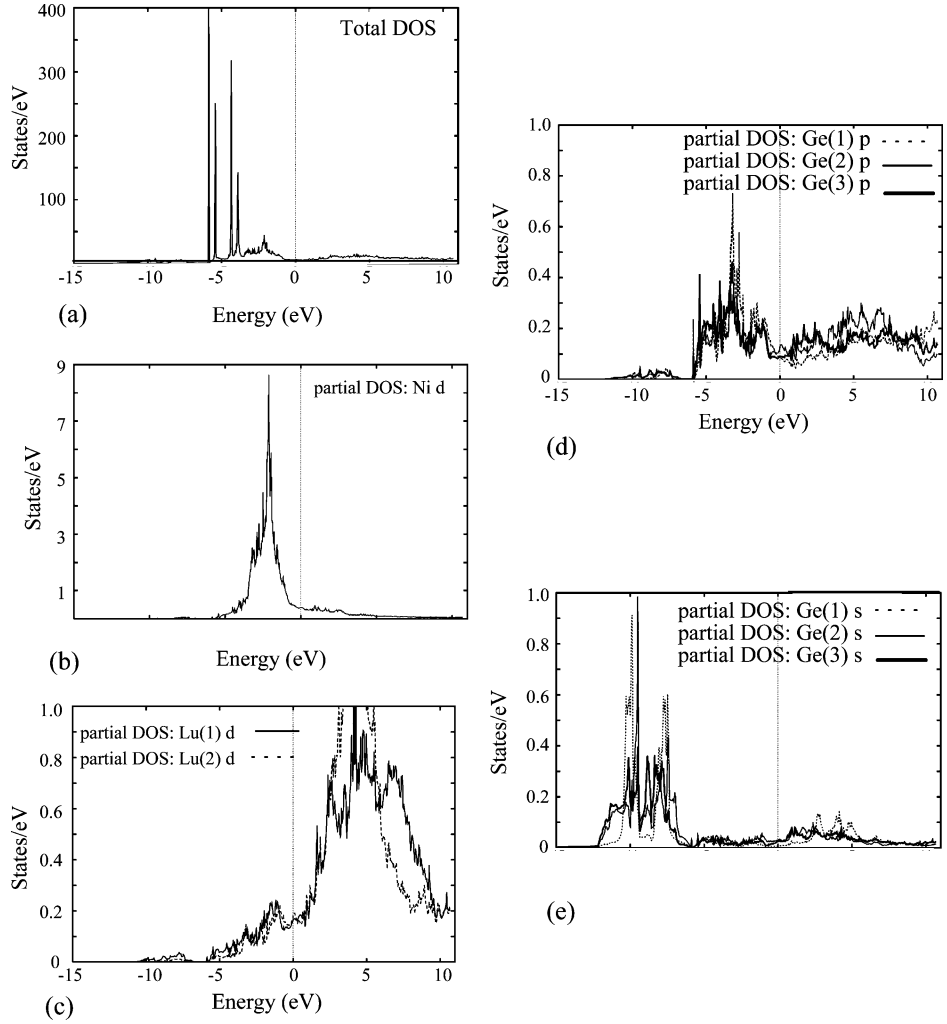

Figure 5. (a) Total DOS for $LuNiGe_2$. (b) Ni d DOS for $LuNiGe_2$. (c) Lu(1) d and Lu(2) d DOS for $LuNiGe_2$. (d) Ge(1) p, Ge(2) p, and Ge(3) p DOS for $LuNiGe_2$. (e) Ge(1) s, Ge(2) s, and Ge(3) s DOS for $LuNiGe_2$.

likely indicates a high barrier to phase transformation, which is consistent with the large amount of bond breaking and reforming required for the two phases to interconvert, which was discussed above.

One final experiment was attempted where the α- and β-forms of the compound were placed in separate alumina tubes and were combined with a 10-fold molar excess of indium and annealed at 950 °C for 2 weeks. This proved successful in interconverting a substantial amount (~50%) of the β-form to the α-form. The α-form was simply recrystallized by the indium to form larger single crystals. This demonstrates that indium indeed acts as a solvent to lower the barrier of activation for interconversion by dissolving the β-phase and recrystallizing it in the α-form.

Band Structure Calculations. Band structure calculations were performed on both the α- and β-form of $LuNiGe_2$ in order to better understand the bonding within the system and to calculate the total energy of each phase. The band structure of the α-form will not be discussed here; rather, we will compare its total energy to that of the β-phase. The calculations suggest that the α-$LuNiGe_2$ is more thermodynamically stable than the β-form by approximately 89 kJ/(mol $LuNiGe_2$). This result is in good agreement with our experimental findings described above. Inspection of the density of states plots for the 2 forms found that the tetrahedally coordinated Ge site of the α-form had p-bands centered at −5 eV. The p-band of the other Ge atom were slightly higher at −2 eV. All the Ge sites in the β-form have p-bands centered at −2 eV. All other bands for the 2 forms fall in the same energy region, so it seems that the stability of α-form has its origins in the tetrahedral coordination of Ge atoms by Ni, a structural feature exclusive to the α-form. The tetrahedral bonding environment alone is not sufficient as Ge(3) in the β-form is also in such an environment. With the difference being that Ge(3) forms a dimer with its symmetry generated equivalent, it therefore must be the exclusive coordination of Ni.

The total calculated density of states (DOS) for β-$LuNiGe_2$ is shown in Figure 5a. Two main features dominate the DOS. The first is the nondispersed f orbital based states of the two crystallographically distinct rare earth sites located between −6 and −4 eV. The second the Ni d states centered at −3 eV. A total of four large narrow f bands appear because each of the two rare earth ion bands are split in two by spin−orbit coupling. These bands are quite low in energy and are therefore not expected to play a role in conduction.

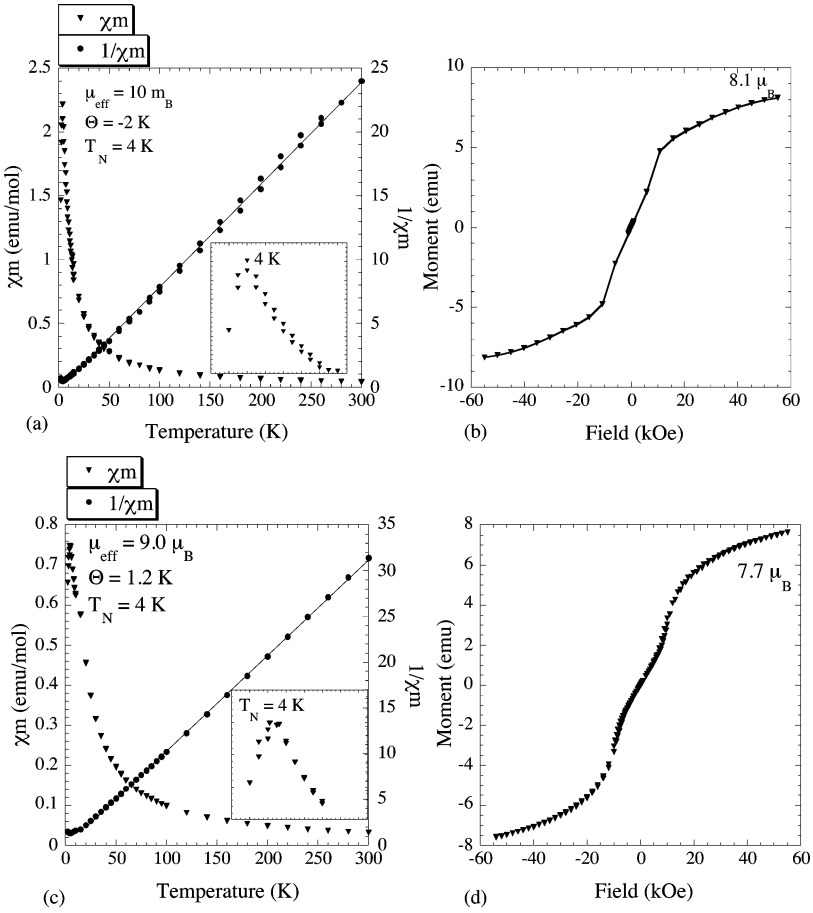

Figure 6. (a) Temperature dependent magnetic susceptibility (χ_m and $1/\chi_m$) for β-DyNiGe$_2$. The inset shows the antiferromagnetic ordering at low temperatures. (b) Magnetization curve for β-DyNiGe$_2$. (c) Magnetic susceptibility (χ_m and $1/\chi_m$) for β-ErNiGe$_2$. The inset shows the antiferromagnetic ordering. (d) Magnetization curve for β-ErNiGe.

The Ni d bands are also located well below the Fermi level and suggest that the Ni atoms have a filled d^{10} electronic configuration, Figure 5b. Therefore, the Ni is essentially reduced to a diamagnetic species. Filled d bands of late transition metals are a common feature in intermetallic compounds containing more electropositive elements.[22]

Also evident from the total DOS plot is that the β-LuNiGe$_2$ is metallic as there are 8 states/eV at the Fermi level. Bands derived from Lu d orbitals lie between 7 and -2 eV indicating that the Lu ions are in a 3+ state as they have transferred their electrons to delocalized orbitals, Figure 5c. The Ge contribution to the density of states is rather small; there are p bands present in all three Ge atoms between -5 and 0 eV allowing for effective overlap between these bands with the d bands of Ni and Lu, Figure 5d. The s bands of the Ge atoms are located at very low energies, between -11 and -6 eV, Figure 5e.

Magnetism. Magnetic measurements performed on β-DyNiGe$_2$ and β-ErNiGe$_2$ show antiferromagnetic ordering with T_N of 4 K for each, Figure 6a,c. Above the Néel temperature, the compounds obey the Curie law. β-YbNiGe$_2$ and β-LuNiGe$_2$ do not show any ordering. Magnetization curves for DyNiGe$_2$ and ErNiGe$_3$ can be seen in Figure 6b,d, respectively; these data show that the antiferromagnetic order is broken by a very small applied field resulting in a metamagnetic transition. The magnetization curve does not saturate for either, and the μ_{sat} for each is approximately 80% of the theoretical value. The measured effective magnetic moment of β-DyNiGe$_2$ is 10.0 μ_B which is close to the value calculated for a Dy^{3+} ion which is 10.6 μ_B.[23] The measured magnetic moment of β-ErNiGe$_2$ was 9.0 μ_B, which compares to the calculated value of Er^{3+} which is 9.6 μ_B. Likewise, β-YbNiGe$_2$ has an effective magnetic moment of 4.65 μ_B, which compares to the theoretical value of 4.56 μ_B.[21] Conversely, β-LuNiGe$_2$ exhibits temperature independent Pauli paramagnetism. These findings are consistent with those predicted from the band structure calculations which showed Ni to be a d^{10} diamagnetic species; therefore, the only contribution to the paramagnetic susceptibility would be from the lanthanide ions. Given these results, we may write the compounds as $RE^{3+}[NiGe_2]^{3-}$.

A great deal of work has been done characterizing the magnetic structure of REIrGe$_2$, REPtGe$_2$, REPdGe$_2$.[11] Many of these compounds have very complex structures including canted antiferromagnetism and incommensurately modulated antiferromagnetism to name a few. Therefore, the magnetic ordering phenomena observed in β-DyNiGe$_2$ and β-ErNiGe$_2$

(22) Vajenine, G. V.; Hoffman, R. *J. Am. Chem. Soc.* **1998**, *120*, 4200.

(23) Kittel, C. *Introduction to Solid State Physics*; 7th ed.; Wiley: New York, 1996; p 425.

are also of interest to search similar effects or even as model compounds for comparison purposes to see what effect a first row transition metal would have on magnetic properties.

In conclusion, we have presented here new forms of the compound $RENiGe_2$ (RE = Er, Dy, Yb, Lu) which crystallize as the $YIrGe_2$ structure type grown from an indium flux. These phases are intriguing, because other phases with the same composition ($RENiGe_2$) have been known for some time, but they crystallize in the $CeNiSi_2$ structure type. What is more, many $REMGe_2$ species with RE = Tb−Lu, Y and M = Pd, Pt, Ir with the $YIrGe_2$ structure type are known, but phases with first row transition metals have not been reported until now. The discovery of these compounds is an excellent example of how a metal flux coupled with the right conditions of temperature and time can alter the reaction outcome and stabilize kinetic phases.

Acknowledgment. Financial support from the Department of Energy (Grant DE-FG02-99ER45793) and the NSF-DMR summer solid state chemistry program for J. R. Gour is gratefully acknowledged. Part of this work was carried out at the Center for Advanced Microscopy and the Center for Sensor Materials at Michigan State University. M.G.K. thanks the Alexander von Humboldt Foundation for a Fellowship.

Supporting Information Available: Tables of crystallographic details, atomic coordinates, isotropic and anisotropic displacement parameters for all atoms, and interatomic distances and angles for $DyNiGe_2$, $ErNiGe_2$, $YbNiGe_2$, and $LuNiGe_2$. This material is available free of charge via the Internet at http://pubs.acs.org.

IC035303J